

Whispering among Brain Cells

James Woessner, M.D., Ph.D.

Advanced Phys Med

Lubbock, Texas

Whispering among Brain Cells*:

The Effect of Electromagnetic Fields Associated with Transcranial Stimulation

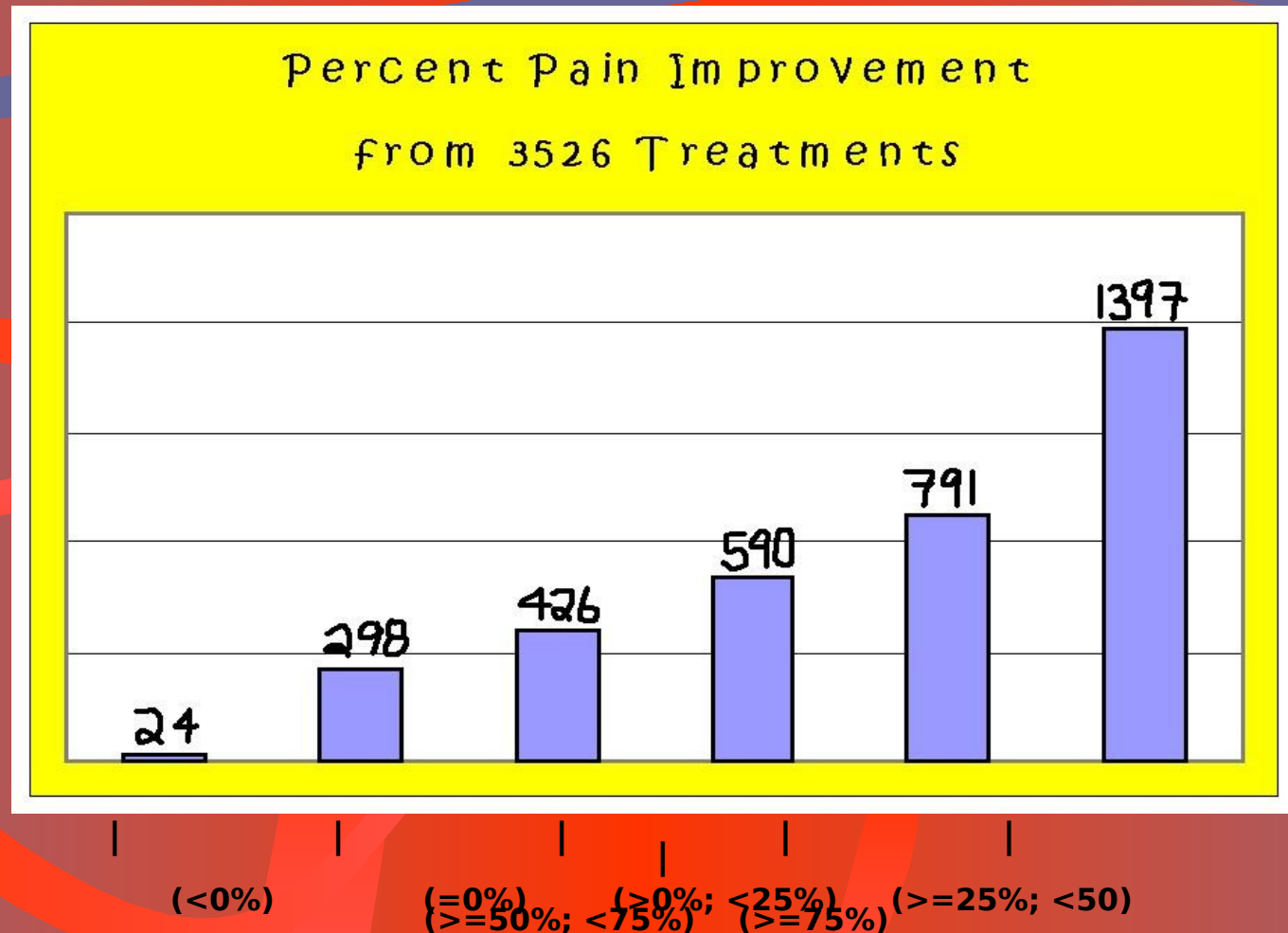
Laboratory animal data and clinical data from human subjects show that transcranial stimulation has a measurable effect on brain and body functions. While the proposition that the secondary electromagnetic field is causative rather than the electrical current itself, at present, is conjecture, we have data to show true intracranial effects of transcranial and body stimulation. The laboratory animal data shows that even with peripheral stimulation there can be clear intracranial waveform changes. Measuring the levels of specific neurotransmitters from human subjects shows undeniable elevations in these substances, and correlate with clinical benefits. Immediate decreases in perceived pain and discomfort as found in clinical data suggest that these intracranial changes have actual effects that are likely caused by electromagnetic forces. These results have tantalizing implications for the effect of electromagnetic energy on human health and well being.

*** — Concept proposed by Dr. Ross Adey.**

Where am I coming from?

- **Physics and Biology major in college.**
- **Ph.D. in Biology.**
- **Neurology training.**
- **Physiatrist specializing in pain treatment.**
- **Over 4000 electric nerve blocks.**
- **Over 300 transcranial stimulation treatments.**
- **The results are much more than placebo.**
- **Electromagnetic fields are it!**

Electric Nerve Blocks



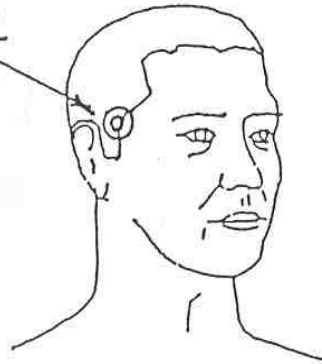
Transcranial Stim Electrode Placement



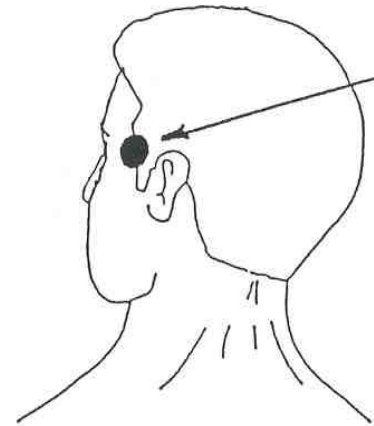
DEPRESSION, SYMPTOM REDUCTION

HEAD---1-10

Red(+)



Black(-)



Liss Transcranial Data

- DB a special case:
 - with an average of 16% average improvement per each of 41 treatments
 - he kept coming back
 - he got a home unit
 - he uses it daily
 - He said yesterday that it is the only thing keeping him alive!

Other Liss Transcranial **Data**

- **Sometimes with other treatments.**
- **57% average improvement for each of 55 treatments in various pains.**
- **Sometimes felt better later.**
- **Mostly just as good alone.**

Randomized Controlled Trials of rTMS in Schizophrenia									
Study # type	Investigator	Year	Site (state/country)	Design	Group	N	Improvement (Decrease in mean HAM-D)	Total %	Depression
2	George-1	1995	Maryland	Open	rTMS	6	28%	156%	1 MDD/5 BMD
4	Kolbinger	1995	Germany	Parallel	rTMS	5	15%	75%	MDD
	"				rTMS	5	34%	170%	
5	Conca	1996	Austria	Parallel	rTMS	12	58%	696%	MDD
6	Pascual-Leone-1	1996	Spain	Crossover	rTMS	17	45%	765%	MDD
8	Grisaru-2	1997	Israel	Open	rTMS	10	26%	260%	6 MDD/3 BMD/1
9	Epstein/Figiel	1998	Georgia	Open	rTMS	32	52%	1664%	29 MDD/3 BMD
10	Figiel/Epstein	1998	Georgia	Open	rTMS	56	43%	2408%	53 MDD/3 BMD
11	Feinsod and Klein	1998	Israel	Open	rTMS	14	31%	434%	MDD
12	Avery	1999	Washington	Parallel	rTMS	4	49%	196%	MDD
13	Klein	1999	Israel	Parallel	rTMS	36	47%	1692%	57 MDD/ 13
14	Loo	1999	Australia	Parallel	rTMS	9	23%	207%	15 MDD/3 BMD
16	Triggs	1999	Florida	Open	rTMS	10	41%	410%	MDD
	"				rTMS	10	20%	200%	
20	Stikhina	1999	Russia	Parallel	rTMS	15	62%	930%	"Neurotic"
21	Padberg	1999	Germany	Parallel	rTMS	6	6%	36%	MDD
	"				rTMS	6	19%	114%	
22	Menkes	1999	Kentucky	Open	rTMS	8	42%	336%	MDD/dysthymia
23	Berman/Boutros	2000	Connecticut	Parallel	rTMS	10	34%	340%	MDD
24	Eschweiler	2000	Germany	Crossover	rTMS	12	22%	264%	MDD
25	George/Nahas	2000	South Carolina	Parallel	rTMS	10	48%	480%	MDD
	"				rTMS	10	28%	280%	
26	Grunhaus	2000	Israel	Open	rTMS	20	40%	800%	MDD
	"				ECT	20	60%	1200%	
27	d'Alfonso/Schouten	NA	Netherlands	Open	rTMS	7	21%	147%	MDD
28	Ebmeier	NA	Scotland	Parallel	rTMS	5	44%	220%	MDD
	"			Parallel	rTMS	5	34%	170%	MDD
	"			Parallel	rTMS	5	46%	230%	MDD
29	Eckert	NA	Germany	Open	rTMS	5	62%	310%	BMD
30	Pascual-Leone-2	NA	Spain	Parallel	rTMS	20	52%	1040%	MDD
33	Avery - 2	NA	Washington	Parallel	rTMS	7	35%	245%	MDD
Total						397	41%	16475%	

Stereotact Funct Neurosurg 1989;53(3):149-56

Long DM, Uematsu S, Kouba RB. Placebo responses to medical device therapy for pain.

Department of Neurosurgery, Johns Hopkins University School of Medicine, Baltimore, Md.

Placebo response to a functionless machine was tested in 58 patients with chronic pain. Thirteen discontinued treatment before the planned trials were complete: 5 did so because sham therapy worsened their pain. Forty-five patients completed three trials of treatment with a magnetic device, one trial of which was a sham. Thirteen percent (13%) of patients undergoing sham therapy experienced relief of pain, improved range of motion, and decrease in muscle spasm. Eleven percent (11%) of the sham trials resulted in significant increase in pain. The placebo/nocebo response to sham therapy with a device is similar to that previously reported for prolonged drug treatment, but is lower than the placebo rate for short-term medication trials.

Magnetic vs. Electric

- **External Generation.**
 - Magnetic
 - Electrical
- **Moving Charges = Current.**
- **Current = EMF.**
- **Magnetic Fields move Charges.**
- **Static or Pulsed Magnetic Fields.**
- **Direct or Indirect (Current).**
- **Both have independent actions.**
- **Hypothesis: EMF is the deal!**

Electric vs. Electromagnetic

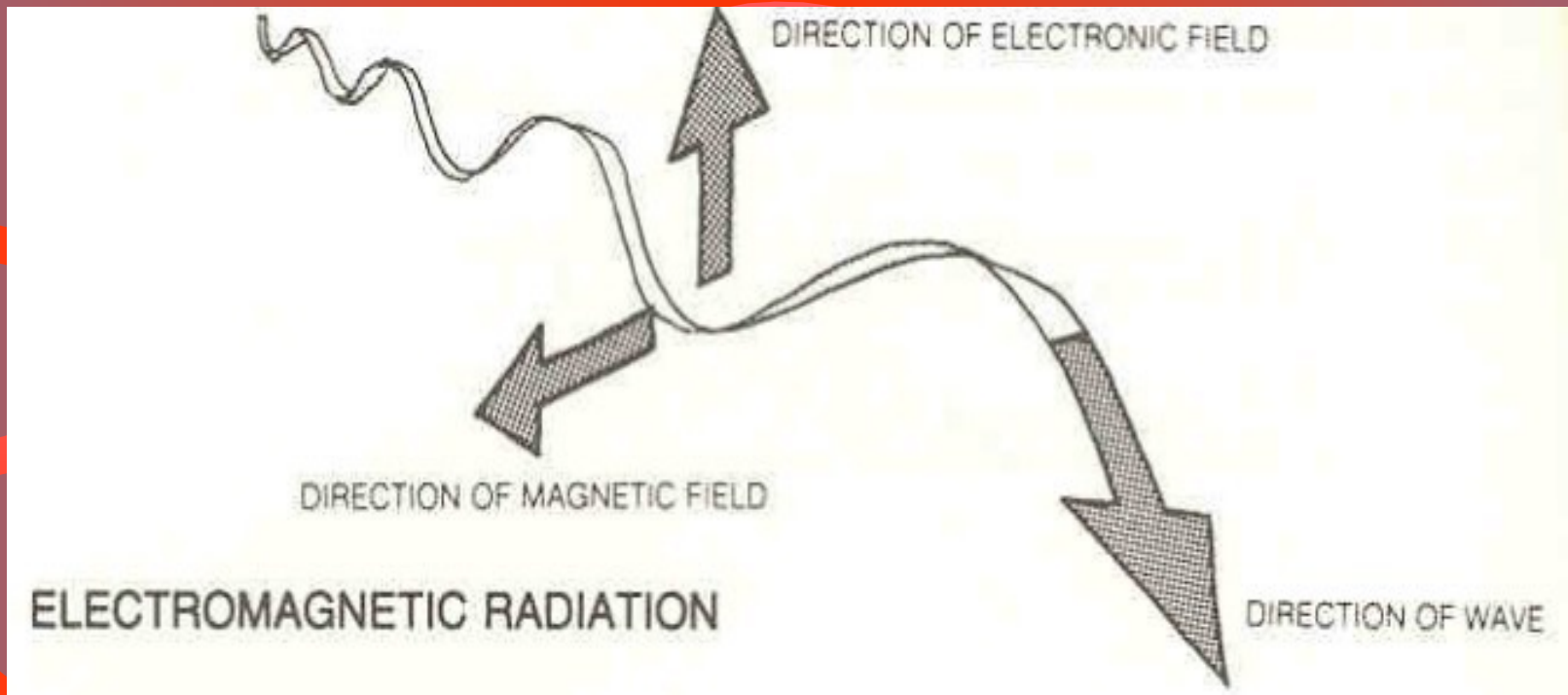
- Electric

- electron flow
- insulation controlled
- follows least resistance/impedance
- unidirectional
- distant influences
- afferent & efferent
- more focused

- Electromagnetic

- from ion flow
- or electron flow
- polarized molecules
- near effects
- locally powerful
- more generalized
- secondary electrical current

The Right Hand Rule

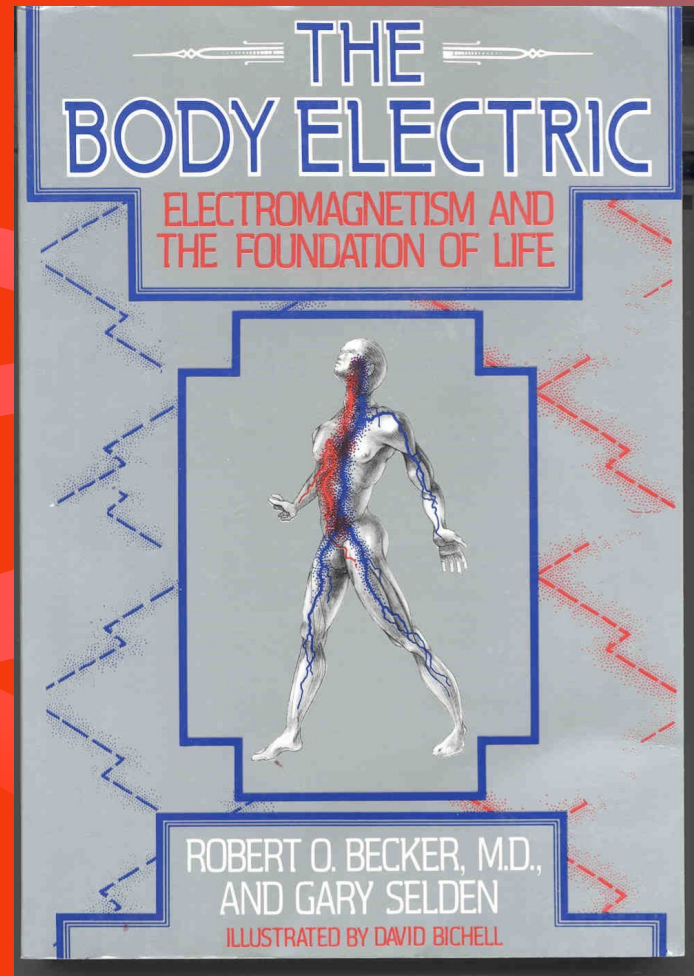
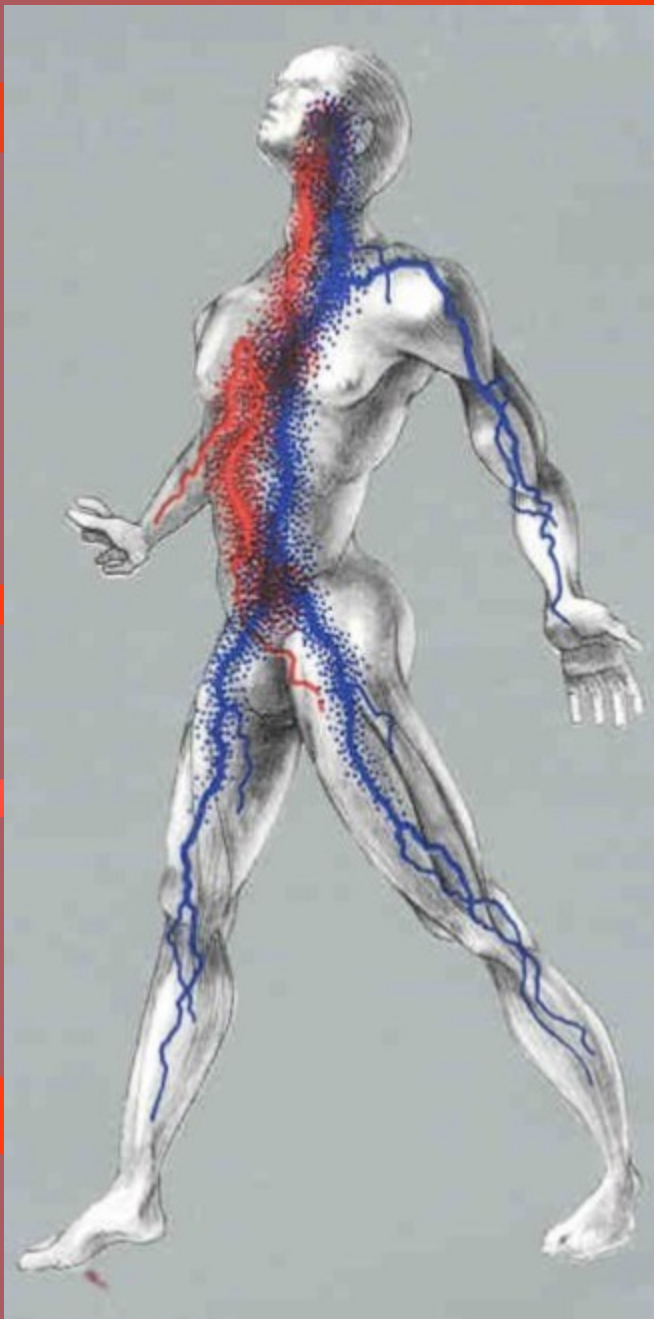


Electrical **Conduction**

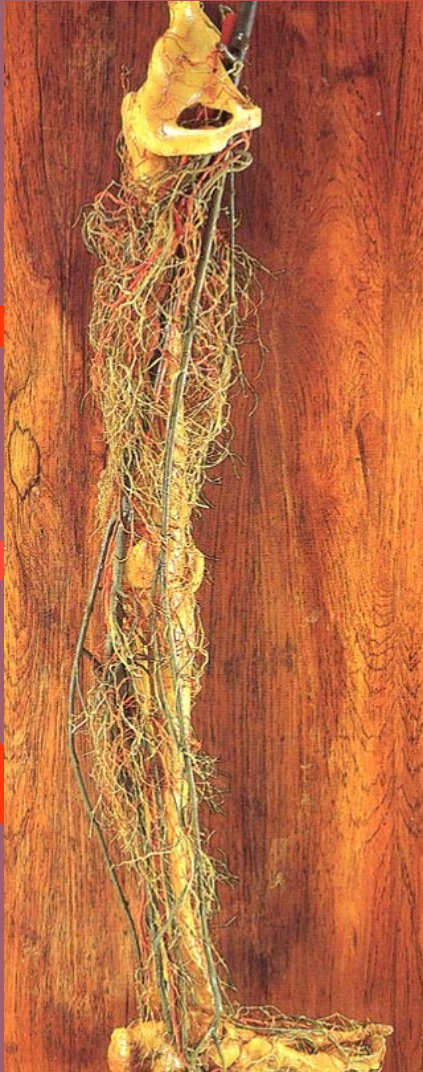
- **Cable theory - uni- or bi-directional**
- **Blood flow**
- **Protoplasmic streaming**
- **Nerve impulses - unicyclical**
- **Ionic movement**
- **Polar molecule movement**
- **Chemical bond dynamics**
- **Shaking phenomenon**
- **Oscillatory phenomenon**

Magnetic Evidence

- **Bacteria**
- **Algae**
- **Birds**
- **Other animals**
- **Humans**



Wires of the Human Body



Nerve Pathways

afferent pathways

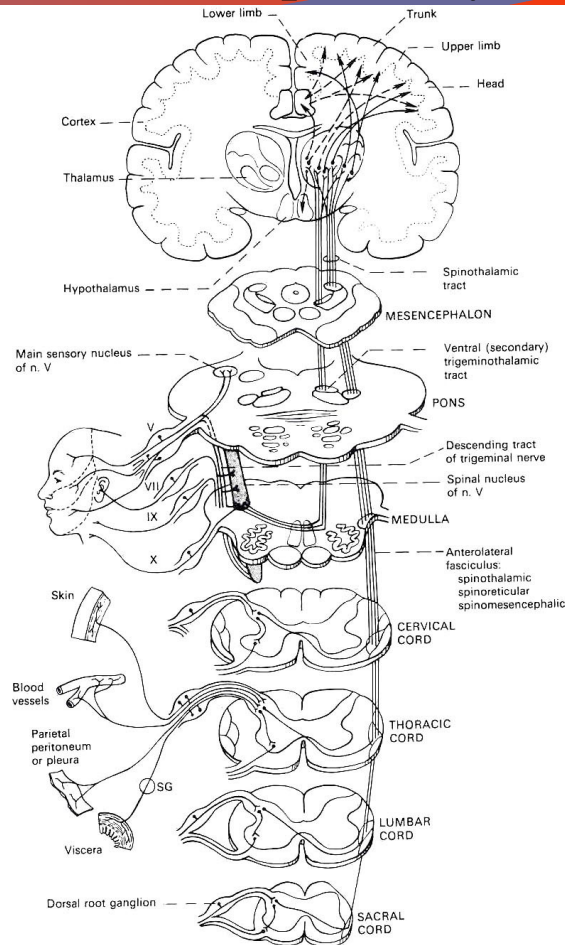
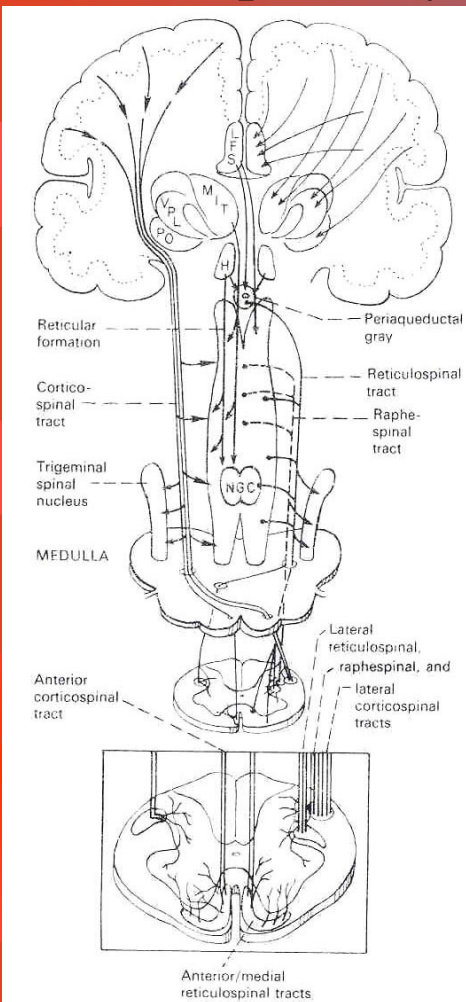
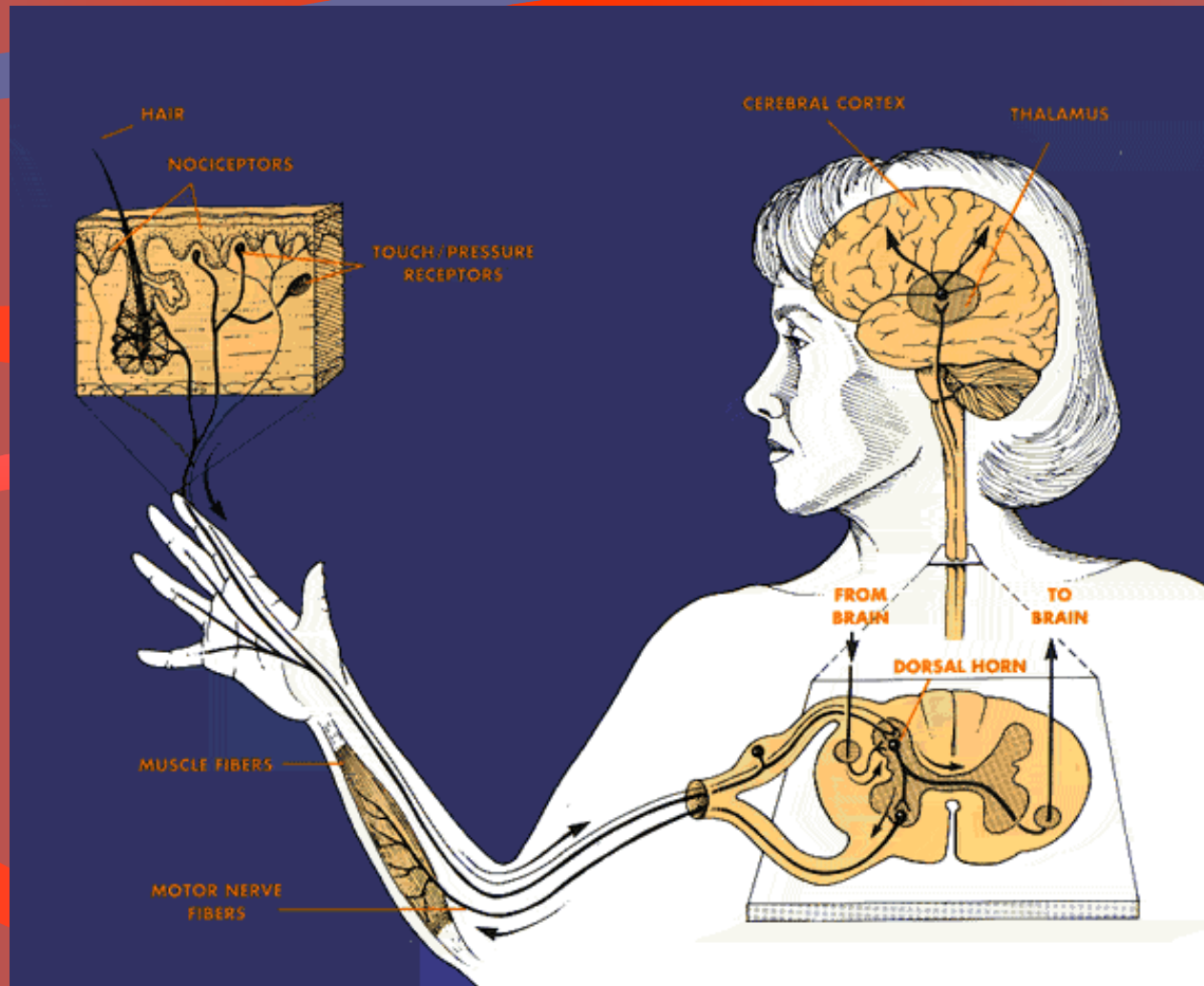


Figure 3-1. Schema of the primary neural pathways for transmission of nociceptive information from various body structures to the brain. The figure forms the basis for detailed discussion of various parts of the pain system in Chapters 3 through 5. (n., nerve; SG, sympathetic ganglion; V, VII, IX, X, cranial nerves.)

efferent pathways



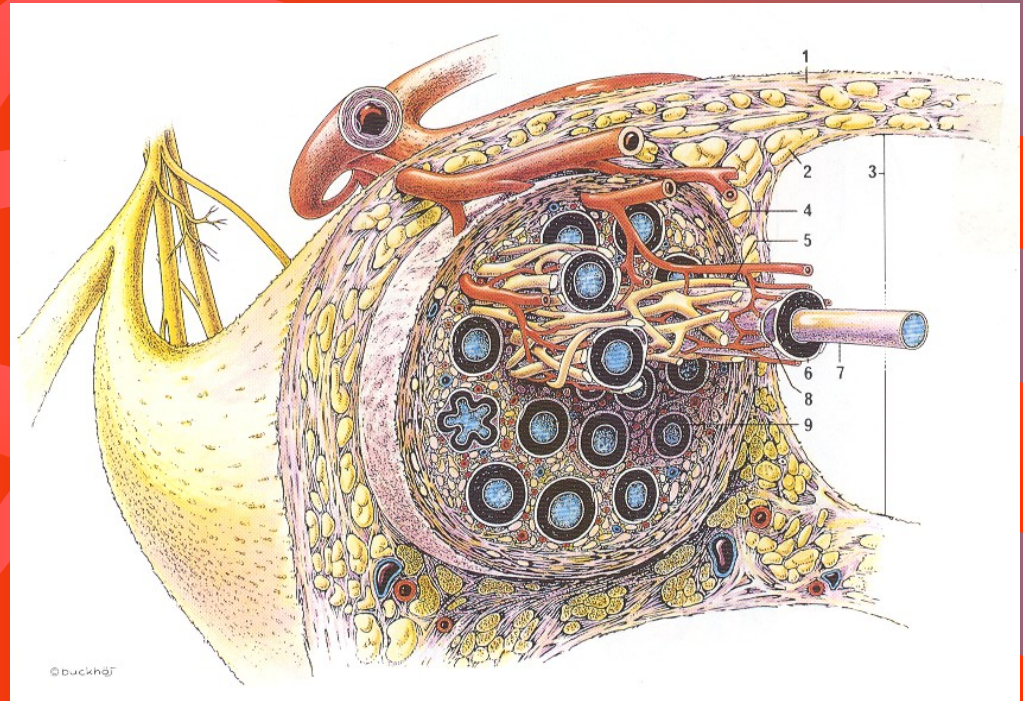
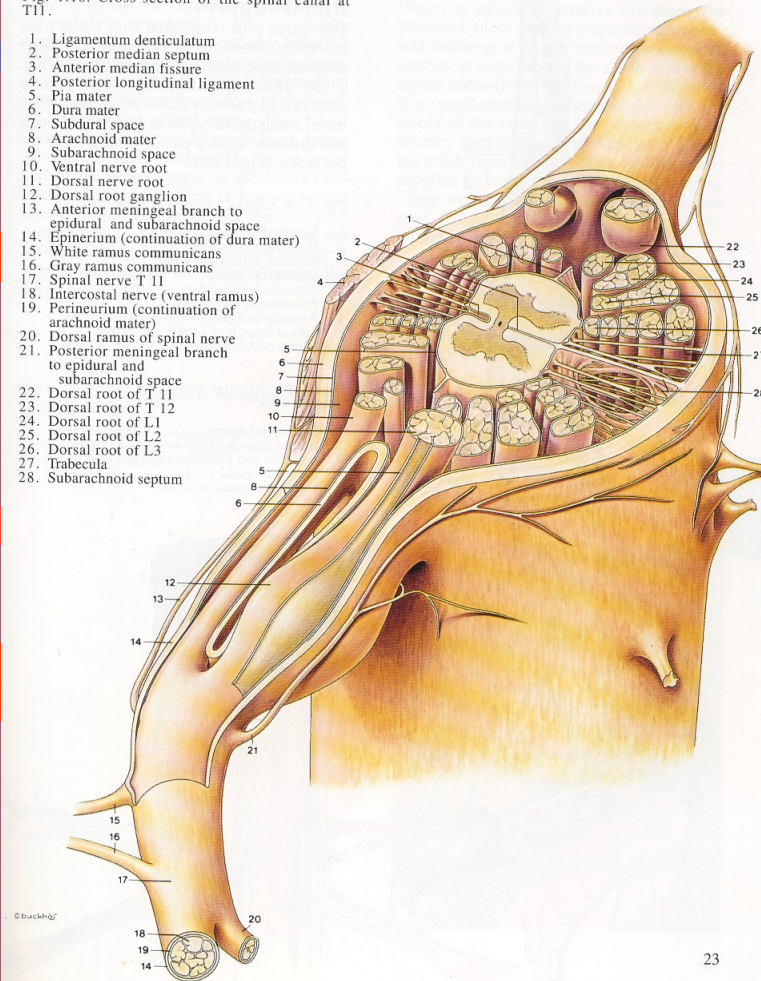
Afferent & Efferent Pain Pathways



Intranerve Organization

Fig. 1.18. Cross-section of the spinal canal at T11.

1. Ligamentum denticulatum
2. Posterior median septum
3. Anterior median fissure
4. Posterior longitudinal ligament
5. Pia mater
6. Dura mater
7. Subdural space
8. Arachnoid mater
9. Subarachnoid space
10. Ventral nerve root
11. Dorsal nerve root
12. Dorsal root ganglion
13. Anterior meningeal branch to epidural and subarachnoid space
14. Epineurium (continuation of dura mater)
15. White ramus communicans
16. Gray ramus communicans
17. Spinal nerve T 11
18. Intercostal nerve (ventral ramus)
19. Perineurium (continuation of arachnoid mater)
20. Dorsal ramus of spinal nerve
21. Posterior meningeal branch to epidural and subarachnoid space
22. Dorsal root of T 11
23. Dorsal root of T 12
24. Dorsal root of L1
25. Dorsal root of L2
26. Dorsal root of L3
27. Trabecula
28. Subarachnoid septum



Peripheral Nervous System Insulation

120

PART ONE NEURAL MEMBRANES

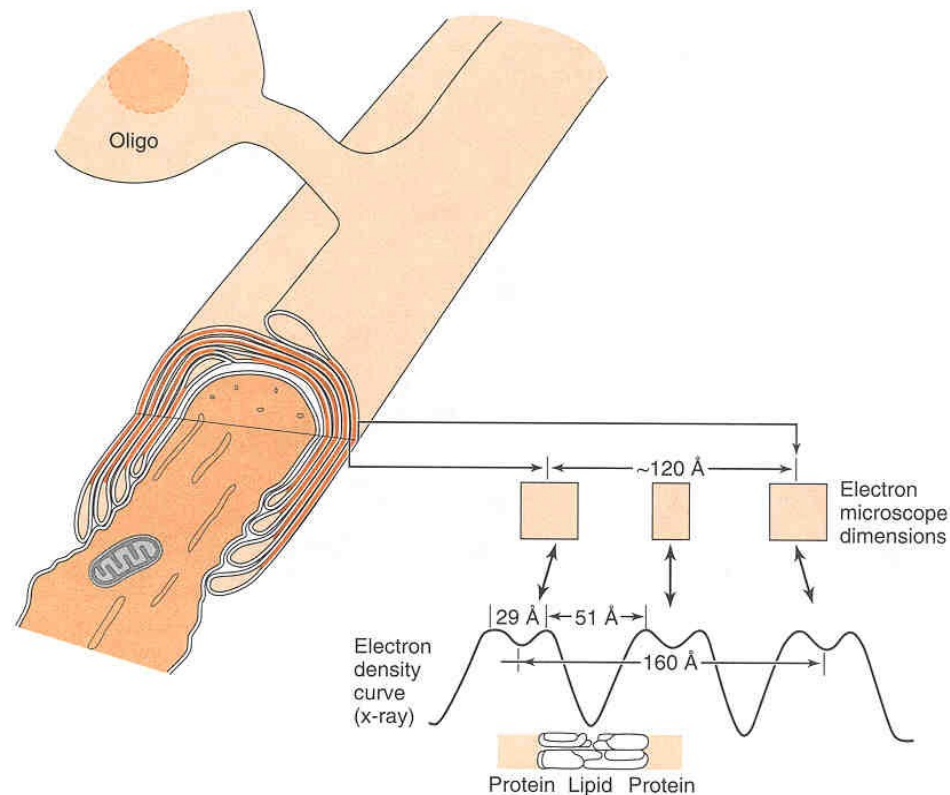
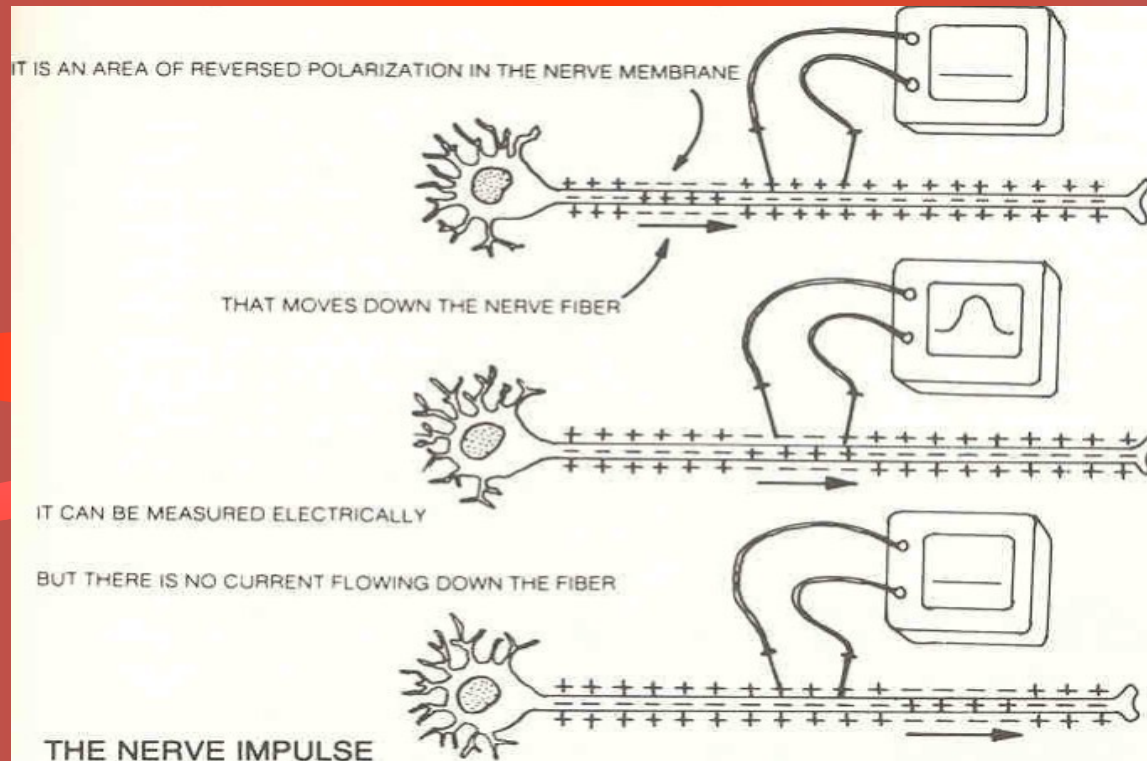


FIG. 3. A composite diagram summarizing some of the ultrastructural data on CNS myelin. At the top an oligodendroglial cell is shown connected to the sheath by a process. The cutaway view of the myelin and axon illustrates the relationship of these two structures at the nodal and paranodal regions. (Only a few myelin layers have been drawn for the sake of clarity.) At the internodal region, the cross section reveals the inner and outer mesaxons and their relationship to the inner cytoplasmic wedges and the outer loop of cytoplasm. Note that in contrast to PNS myelin, there is no full ring of cytoplasm surrounding the outside of the sheath. The lower part of the figure shows roughly the dimensions and appearance of one myelin repeating unit as seen with fixed and embedded preparations in the electron microscope. This is contrasted with the dimensions of the electron density curve of CNS myelin obtained by X-ray diffraction studies in fresh nerve. The components responsible for the peaks and troughs of the curve are sketched below. (From Norton [4]. Reprinted courtesy of Lea & Febiger, publishers.)

Evidence



Bernstein's hypothesis has been confirmed in all important respects, although it remains a hypothesis because no one has yet found what gives the membrane the energy to pump all those ions back and forth. Soon it was broadened, however, to include an explanation of the current of injury. Reasoning that all cells had transmembrane potentials, Bern-

Axonal Transport

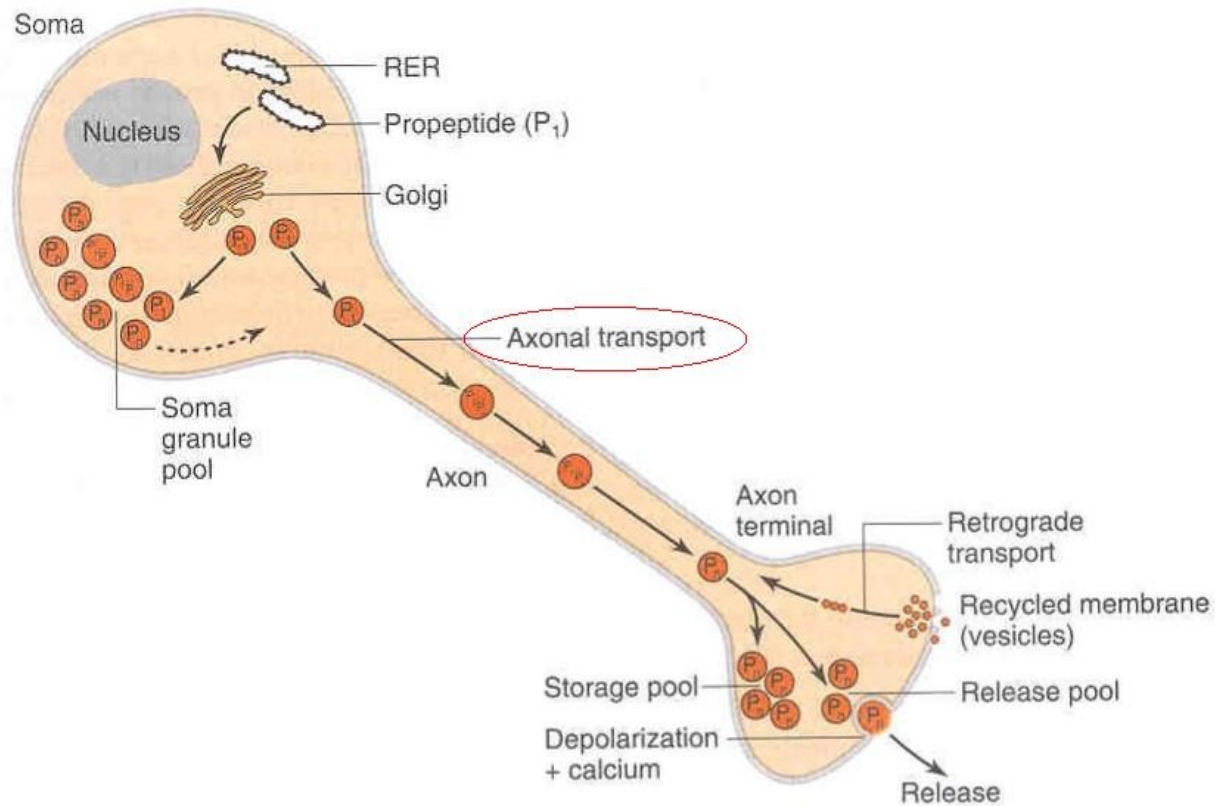


FIG. 6. Hypothetical model of biosynthesis, translocation, processing, and release of peptides in a peptidergic neuron. (RER) rough endoplasmic reticulum; (P_1) propeptide or precursor molecule; ($P_1 \dots P_n$) intermediates between P_1 and P_n ; (P_n) final peptide product of processing. (From Gainer et al. [32].)

Charge Conduits

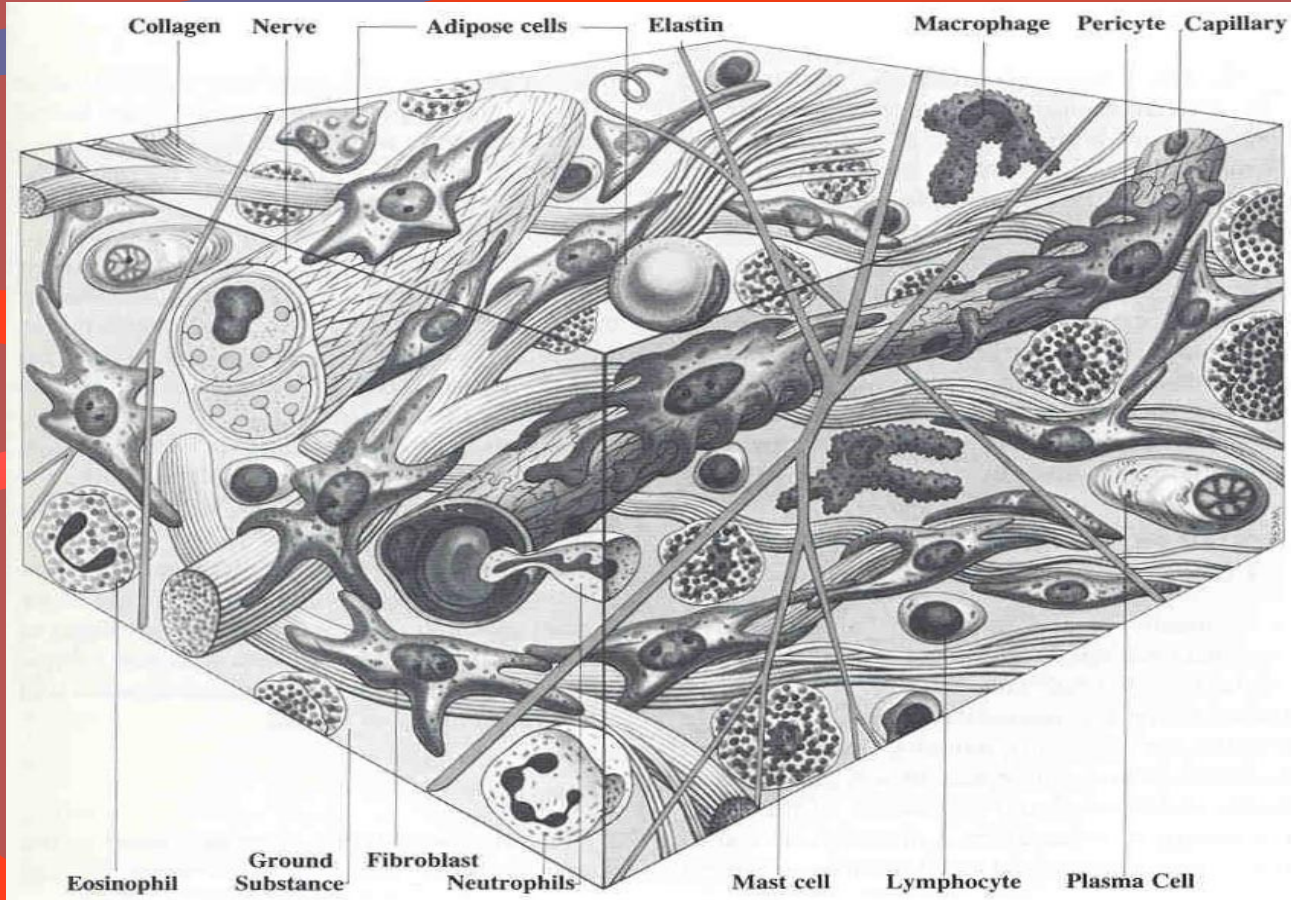


Figure 3-1 A diagrammatic representation of loose connective tissue, showing fibers, cells, ground substance, nerve, and blood vessels. *Source:* Reprinted from *Gray's Anatomy*, ed 35 (p 32) by P. Williams and R. Warwick with permission of W.B. Saunders, © 1973.

Neurons

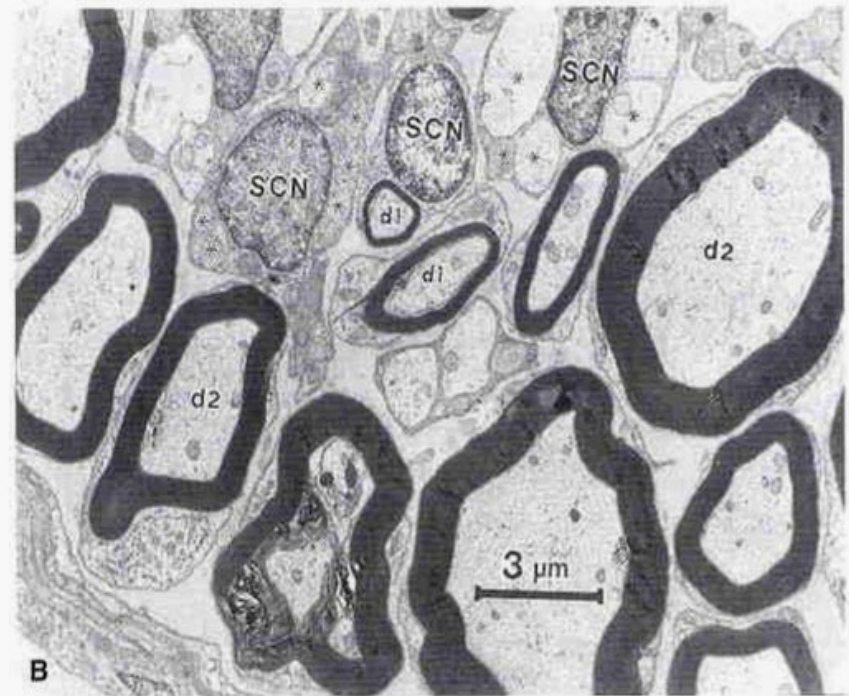
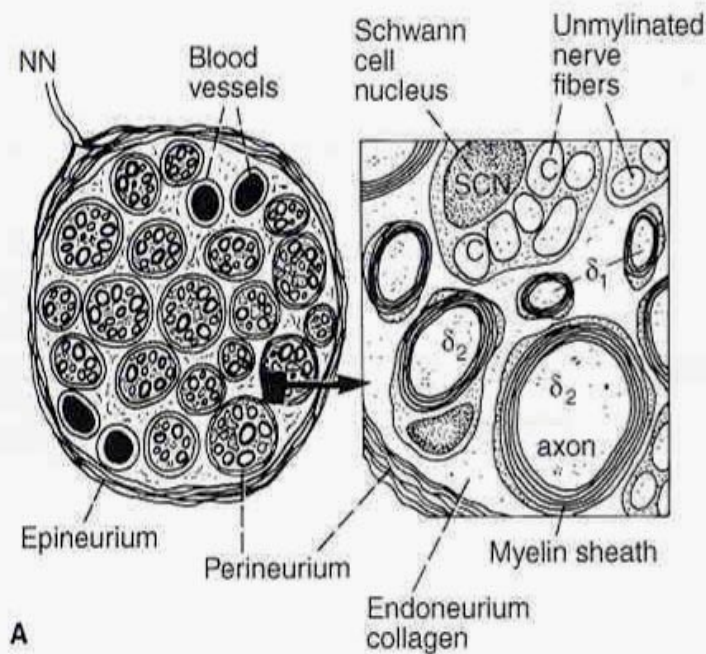


Figure 3-5. **A:** Diagram of a cross-sectioned peripheral nerve showing the many fascicles, each with its own endoneurium collagen and perineurium sheath. The whole nerve has its own innervation of epineurium and vasculature by the nervi nervorum (NN). The higher magnification panel shows details of the ensheathing Schwann cells and their nucleus (SCN) for groups of unmyelinated (C) axons or for single myelinated axons. The A- δ axons can be thin and slow (δ_1) or larger and faster (δ_2). **B:** This electron micrograph of tibial nerve of rat shows a variety of myelinated axon sizes, including small (δ_1) and larger (δ_2) A- δ fibers, and some bundles of unmyelinated C fibers of various sizes (*). Some of the Schwann cell nuclei are indicated (SCN) (magnification, $\times 7,000$; scale, 3 μ m).

Blood Brain Barrier

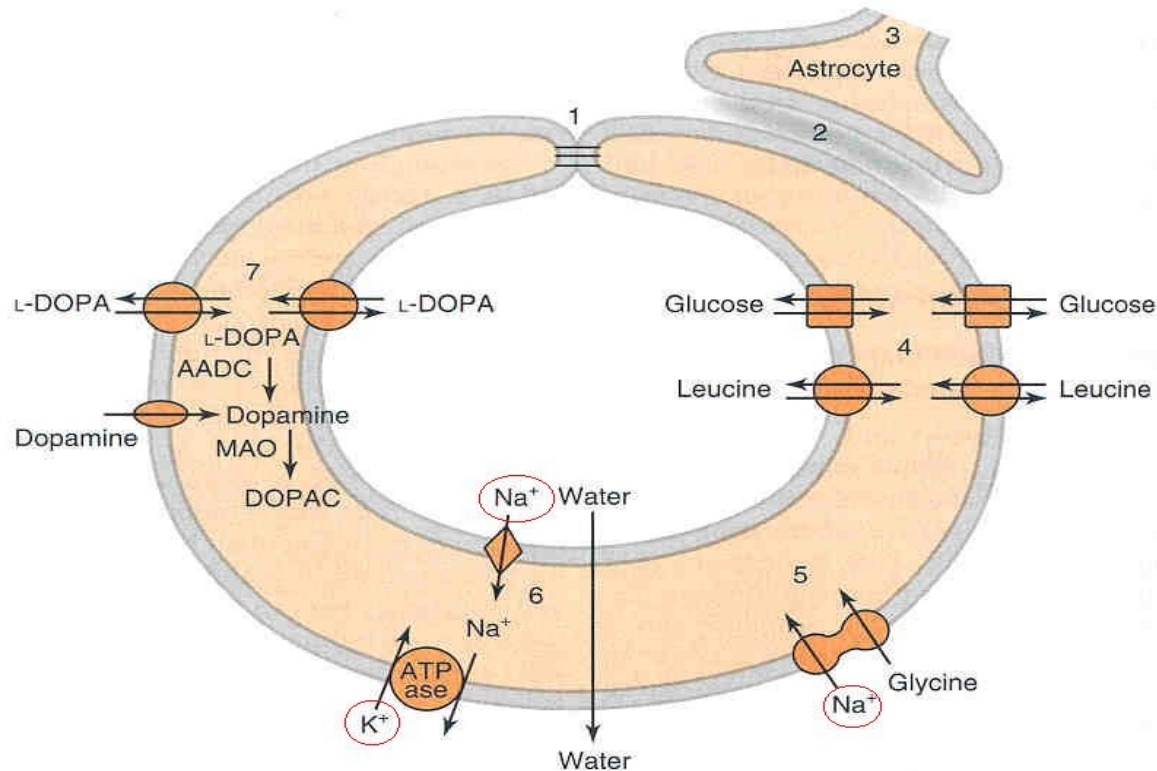


FIG. 1. Schematic diagram of brain capillary. The continuous tight junctions (1) that join endothelial cells in brain capillaries limit the diffusion of large and small solutes across the blood-brain barrier. The basement membrane (2) provides structural support for the capillary and, along with the astrocytic foot processes (3) that encircle the capillary, may influence endothelial cell function. Transport carriers (4) for glucose and essential amino acids facilitate the movement of these solutes into brain, while secondary transport systems (5) appear to cause the efflux of small, nonessential amino acids from brain to blood. Sodium ion transporters on the luminal membrane and Na,K-ATPase on the antiluminal membrane (6) account for the movement of sodium from blood to brain, and this may provide an osmotic driving force for the secretion of interstitial fluid by the brain capillary. The enzymatic blood-brain barrier (7) consists of the uptake of neurotransmitter precursors such as L-DOPA into the endothelial cells via the large neutral amino acid carrier, and their subsequent metabolism to 3,4-dihydroxyphenylacetic acid (DOPAC) by aromatic amino acid decarboxylase (AADC) and monoamine oxidase (MAO) present within the endothelial cell. Neurotransmitters in the interstitial fluid may also be accumulated and metabolized by the brain capillary.

Charged Flow in and out of a Cell

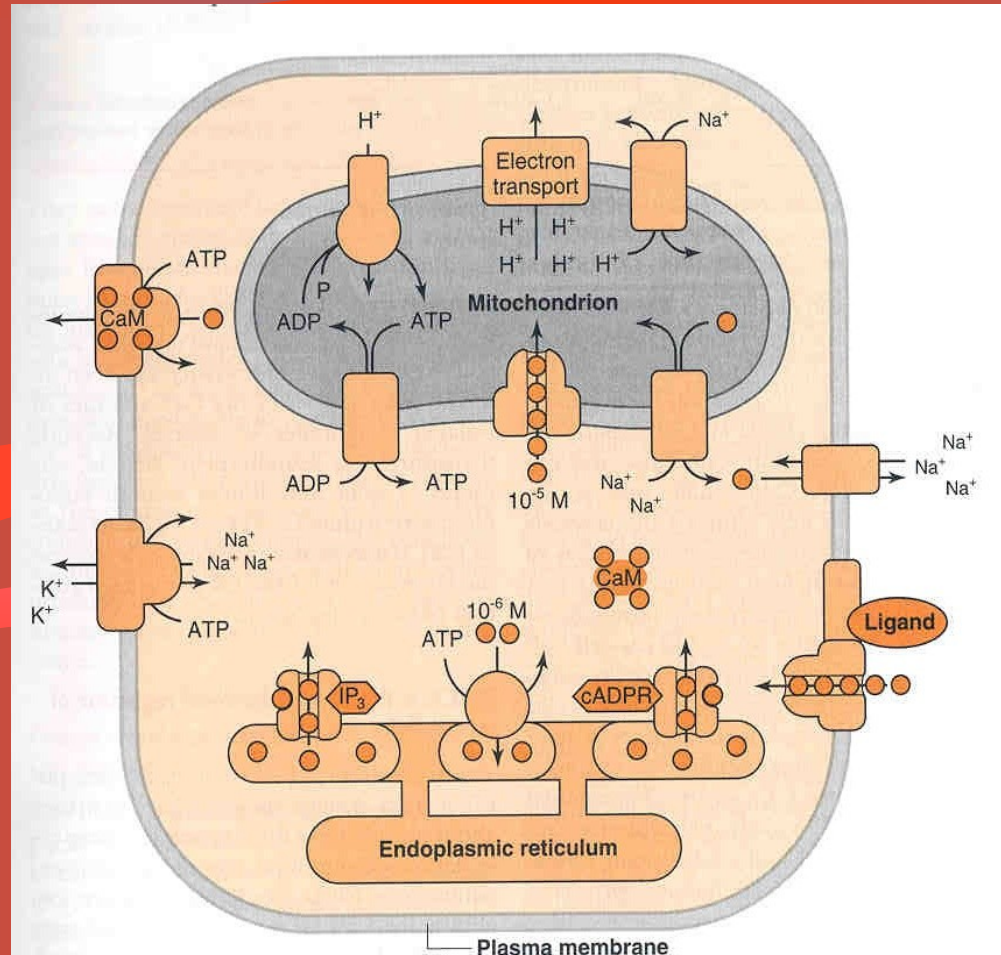


FIG. 6. Ca²⁺ homeostasis. Ca²⁺ enters cells through a variety of ligand- and voltage-regulated channels, but intracellular free Ca²⁺ is normally maintained at less than micromolar levels. Intracellular Ca²⁺ is probably regulated coordinately by a Na⁺/Ca²⁺ antiporter in plasma membranes and by several different Ca-ATPases in plasma membranes and endoplasmic reticulum. The driving force for Na⁺/Ca²⁺ antiporter exchange is the inwardly directed Na⁺ gradient which is maintained by the Na,K-ATPase. Mitochondria may participate transiently in Ca²⁺ homeostasis if the capacities of these other systems are exceeded. Internal stores of Ca²⁺ may be released from endoplasmic reticulum through the action of second messengers, such as IP₃ or Ca²⁺ itself, in response to various receptor systems.

Gap Junctions

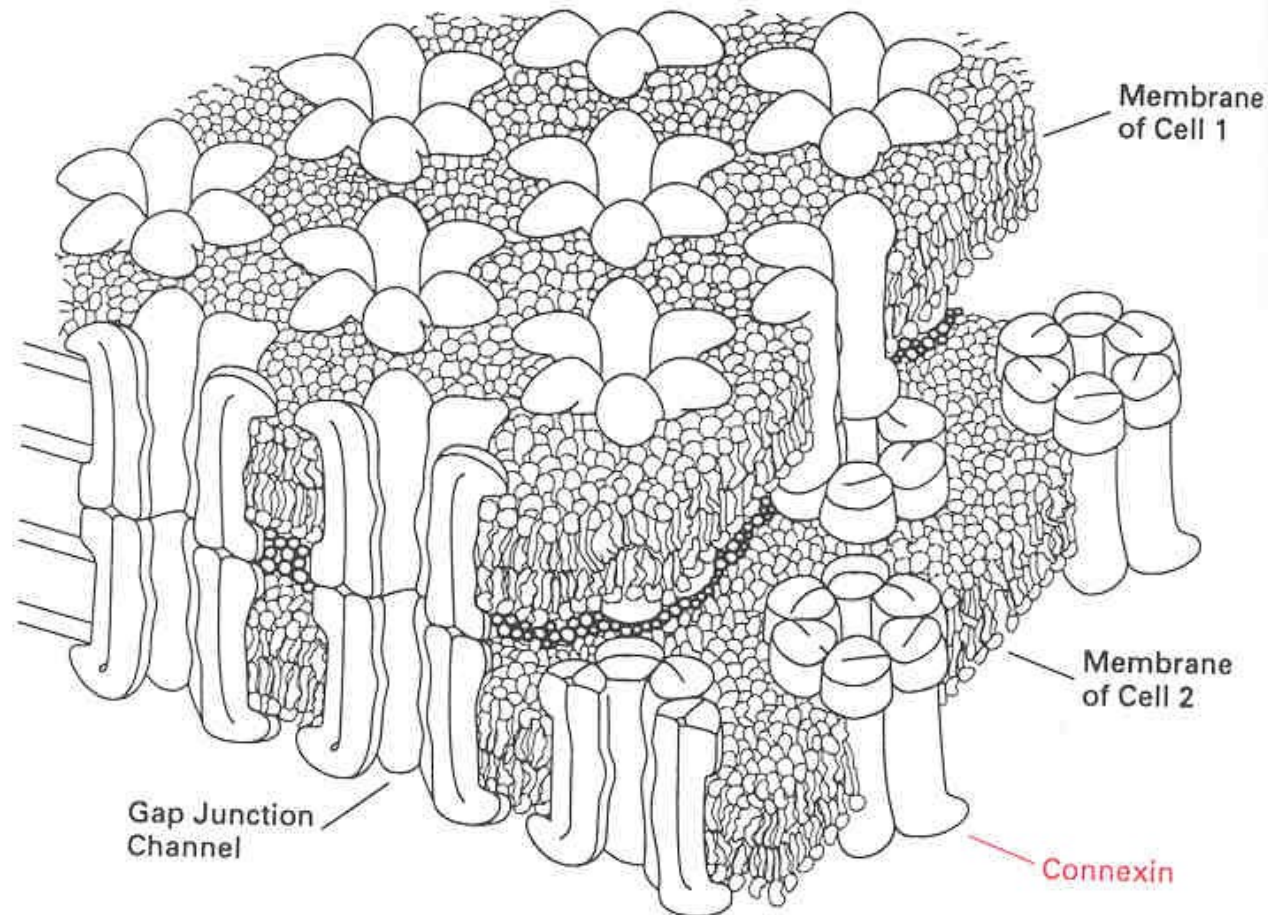


Figure 7-1. Gap junctions. Pores spanning two cell membranes are made of connexin proteins. This picture evolved from the X-ray diffraction work of Makowski et al. (1977).

Molecular Magnets

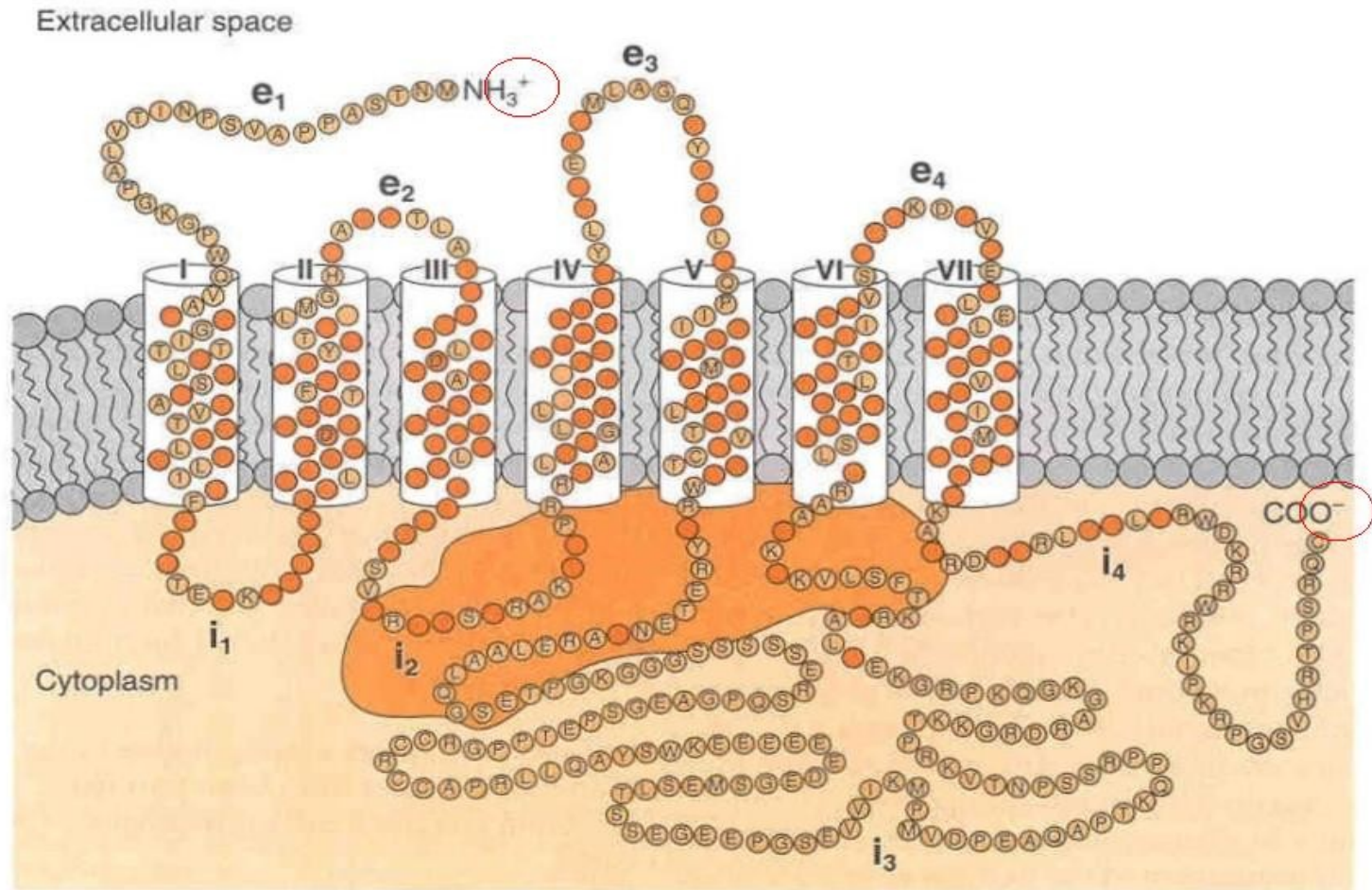
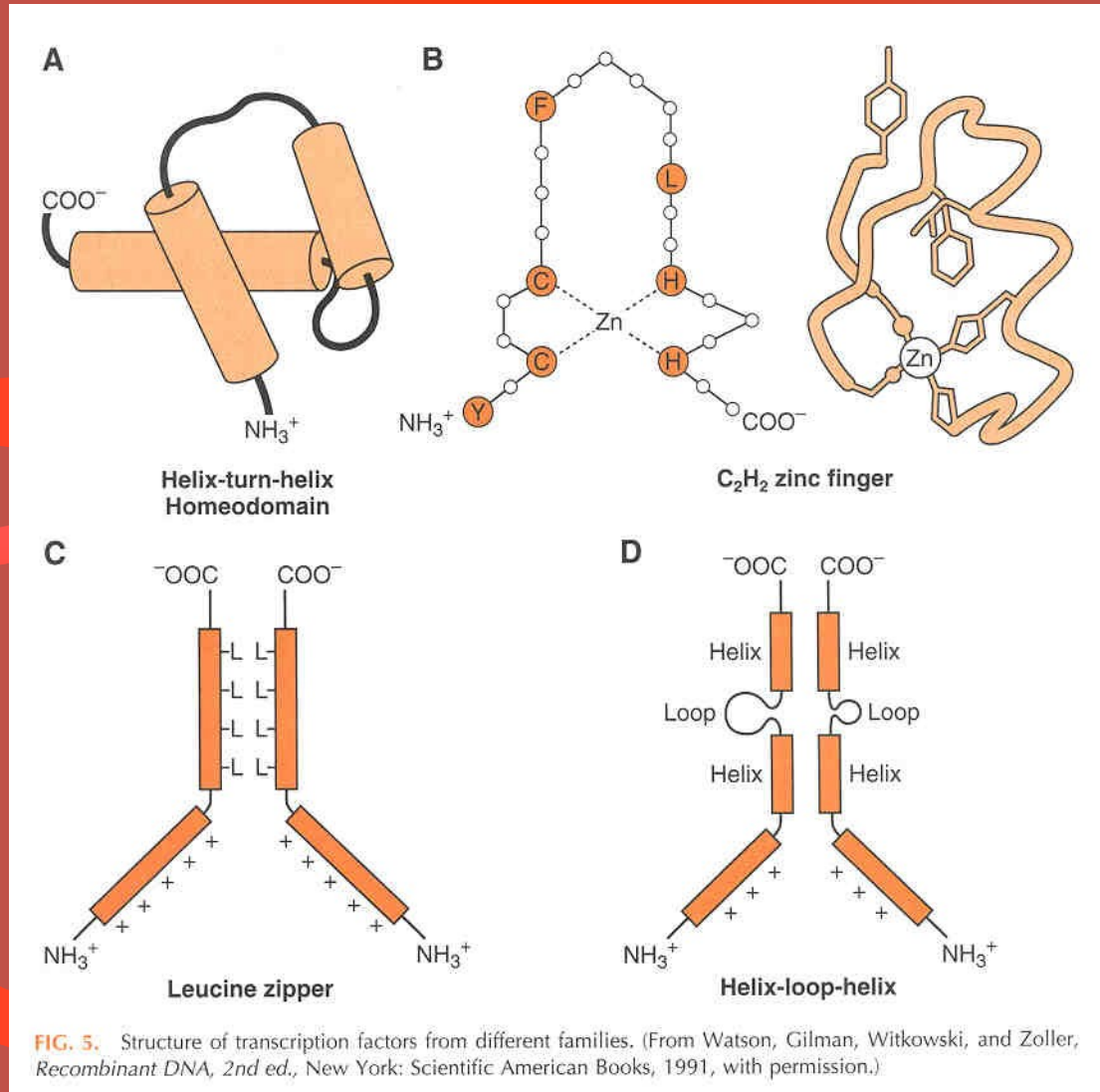


FIG. 10. Predicted amino acid sequence and transmembrane domain structure of the human M₁ muscarinic receptor. Amino acids that are identical among the M₁, M₂, M₃, and M₄ receptors are darkened. The shaded cloud represents the approximate region that determines receptor-G-protein coupling.

Polar Molecules



Ion Transport

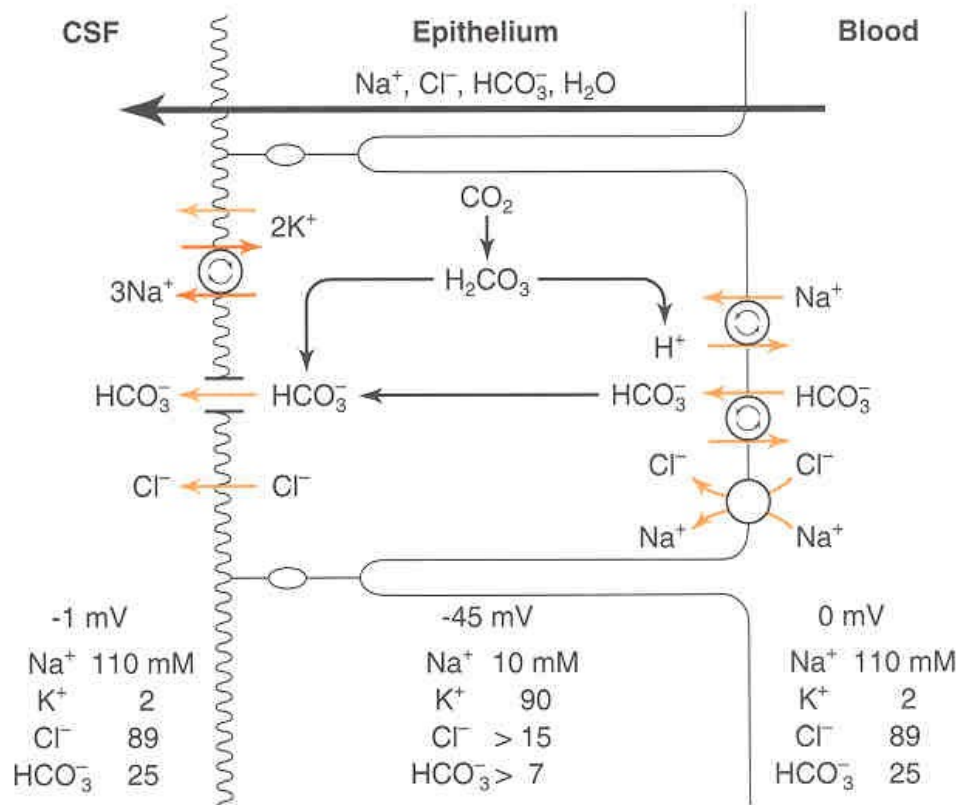


FIG. 7. Schematic diagram of ion transport mechanisms in the choroid plexus epithelial cell. Net transport of Na^+ , Cl^- , and HCO_3^- across the choroid plexus epithelium results in the secretion of CSF. (From Saito and Wright [26]).